

sym-oxepin oxide (**1**) in aprotic solvents (CDCl₃, CH₂Cl₂, CD₂Cl₂, THF, or CH₃CN) with catalytic amounts of MeSO₃H led within seconds to the generation of **13**. In CDCl₃ the addition of MeSO₃H (0.1 mol %) catalyzes the quantitative (¹H NMR) rearrangement of **1** to **13**: ir (CDCl₃) 1725, 1680, 1620, 1260 cm⁻¹; ¹H NMR (CDCl₃, 100 MHz) δ 9.51 (1 H, d), 6.50 (2 H, m), 4.90 (2 H, m), 3.64 (1 H, m); uv (CH₃CN) λ_{max} 246 (ε 590), 310 (110); mass spectrum (70 eV) *m/e* parent 110, base 81. Exact mass of *p*-nitrophenylhydrazone: calcd for C₁₂H₁₁N₃O₃, 245.0800; found, 245.0797.

Reduction of 13 to 4-Hydroxymethyltetrahydropyran (15). The catalytic reduction of **13** to 4-hydroxymethyltetrahydropyran (**15**) was achieved in THF-EtOH over Raney nickel catalyst. The catalyst was prepared as for the reduction of **1** to **14**, except that the metal was both washed and stored under EtOH rather than THF.

sym-Oxepin oxide (**1**) used for the preparation of **13** was generated from azo compound **10** (150.2 mg, 1.09 mmol) by the dissolution and warming of **10** to ambient temperature in THF (4.7 ml). To the solution of **1** was added 2% MeSO₃H in Et₂O (23 μl); the mixture was stirred for 23 min. A portion of CaCO₃ (Merck, precipitated) (41 mg) was added and the suspension was stirred briefly and filtered with an EtOH (4.7 ml) rinse. To the resulting solution of **13** was added a Raney nickel-EtOH slurry (120 μl); the mixture was shaken under H₂ (47 psig) for 40 h. Filtration of the reaction mixture through Celite with an Et₂O rinse, evaporation of the solvents (Vigreux column-steam bath), and preparative gas-liquid chromatography (8 ft X 0.25 in. Carbowax 20M, 10% on 80-100 Diatoport S, 157 °C) gave 4-hydroxymethyltetrahydropyran (**15**) (104.8 mg, 83% based on **10**). The sample of **15** produced by catalytic reduction of **13** was found to be identical with an authentic sample²¹ by GLC coinjection (Carbowax 20M and SE-30), by mixture melting point of the phenylurethane derivatives, and by comparison of the ir, ¹H NMR, and mass spectra. Exact mass of **15** prepared via **13**: calcd for C₆H₁₂O₂, 116.0837; found, 116.0840.

Acknowledgments. I am indebted to Professor R. B. Woodward for his generous support and guidance and to Professor J. E. Baldwin for his valuable discussions and continuing interest. I gratefully acknowledge an NSF predoctoral fellowship (1972-1975).

References and Notes

- Address correspondence to this author at the Department of Chemistry, Massachusetts Institute of Technology, Cambridge, Mass. 02139.
- Reviews: (a) E. Vogel and H. Günther, *Angew. Chem., Int. Ed. Engl.*, **6**, 385 (1967); (b) J. W. Daly, D. M. Jerina, and B. Witkop, *Experientia*, **28**, 1129 (1972); (c) D. M. Jerina, H. Yagi, and J. W. Daly, *Heterocycles*, **1**, 267 (1973); (d) D. M. Jerina and J. W. Daly, *Science*, **185**, 573 (1974).
- W. H. Rastetter, *J. Am. Chem. Soc.*, **97**, 210 (1975).
- H. Klein and W. Grimme, *Angew. Chem., Int. Ed. Engl.*, **13**, 672 (1974).
- (a) N. Neuss, R. Nagarajan, B. B. Molloy, and L. L. Huckstep, *Tetrahedron Lett.*, 4467 (1968); (b) N. Neuss, L. D. Boeck, D. R. Brannon, J. C. Cline, D. C. DeLong, M. Gorman, L. L. Huckstep, D. H. Lively, J. Mabe, M. M. Marsh, B. B. Molloy, R. Nagarajan, J. D. Nelson, and W. M. Stark, *Antimicrob. Agents Chemother.*, 213 (1968).
- See D. D. Haas and W. H. Rastetter, *J. Am. Chem. Soc.*, following paper in this issue, and references cited therein.
- H. O. House, "Modern Synthetic Reactions", 2d ed, W. A. Benjamin, Menlo Park, Calif., 1972, pp 314-315.
- See, e.g., G. J. Kasperek and T. C. Bruice, *J. Am. Chem. Soc.*, **94**, 198 (1972).
- A sample was kindly provided by Dr. W. T. Borden and Y. C. Toong. Later a literature preparation appeared: D. Mackay, C. W. Pilger, and L. L. Wong, *J. Org. Chem.*, **38**, 2043 (1973).
- The stereochemical assignment is corroborated by an isotopic labeling study (see ref 6) which indicates that the epoxide fused anti with respect to the azo bridge of **10** is derived from the epoxide of benzene oxide.
- Y. Kishi, M. Aratani, H. Tanino, T. Fukuyama, T. Goto, S. Inoue, S. Sugiura, and H. Kakoi, *J. Chem. Soc., Chem. Commun.*, 64 (1972).
- Determined from a single kinetic run by the ¹H NMR method described in ref 6; error limit is the standard deviation determined by least-squares fitting of the values of **10** at eight times during the nitrogen extrusion reaction.
- (a) S. Masamune and N. T. Castellucci, *J. Am. Chem. Soc.*, **84**, 2452 (1962); (b) J. Strating, J. H. Keijer, E. Molenaar, and L. Brandsma, *Angew. Chem., Int. Ed. Engl.*, **1**, 399 (1962).
- An extensive treatment of the ¹H NMR spectrum of **1** is given in ref 6.
- High-temperature ¹H NMR spectra were determined in CDCl₂CDCl₂ solution; thermal instability of **1** prevents observation at higher temperatures.
- The rate of the Cope rearrangement for the *sym*-oxepin oxide system has been measured by an isotopic labeling study; see ref 6.
- J. M. Brown, B. T. Golding, and J. J. Stofko, Jr., *J. Chem. Soc., Chem. Commun.*, 319 (1973).
- (a) E. L. Stogryn, M. H. Gianni, and A. J. Passannante, *J. Org. Chem.*, **29**, 1275 (1964); (b) J. C. Pommelet, N. Manisse, and J. Chucho, *Tetrahedron*, **28**, 3929 (1972).
- W. Grimme and K. Seel, *Angew. Chem., Int. Ed. Engl.*, **12**, 507 (1973).
- S. Olsen and R. Bredoch, *Chem. Ber.*, **91**, 1589 (1958).
- A. Burger, L. B. Turnbull, and J. G. Dinwiddie, Jr., *J. Am. Chem. Soc.*, **72**, 5512 (1950).
- A similar procedure utilizing potassium *tert*-butoxide in Et₂O at 0 °C was kindly provided by Dr. W. Lever.
- The Diels-Alder addition is exothermic; ice bath cooling was utilized in large-scale preparations of adduct **7**.
- The use of *p*-nitroperoxybenzoic acid achieves the epoxidation of **7** under significantly milder conditions than those required with *m*-chloroperoxybenzoic acid; *m*-chloroperoxybenzoic acid gave tarry reaction products requiring tedious chromatographic purification and gave yields of **8** not exceeding 30%.
- Adequate shielding should be used during high-temperature epoxidation by *p*-nitroperoxybenzoic acid and the reaction temperature should be carefully regulated; D. F. Debenham, A. J. Owen, and E. F. Pembbridge, *J. Chem. Soc. B*, 213 (1966), report that *p*-nitroperoxybenzoic acid, as the solid, in the absence of radical inhibitors, detonates at 100 °C.
- The activated zinc was protected from contact with air during all manipulations.
- The reductive cleavage products are assumed to include zinc salts and the hydrazinium acetate salt corresponding to azo diepoxide **10**.

Proton Magnetic Resonance Studies of *sym*-Oxepin Oxide

Daniel D. Haas and William H. Rastetter*¹

Contribution from the Department of Chemistry, Harvard University, Cambridge, Massachusetts 02138, and the Department of Chemistry, Massachusetts Institute of Technology, Cambridge, Massachusetts 02139. Received April 9, 1976

Abstract: Proton magnetic resonance studies have yielded information concerning the conformation and the degenerate Cope rearrangement of *sym*-oxepin oxide (**1**). Proton-proton coupling constants derived from a computer simulation of the high-resolution ¹H NMR spectrum of **1** indicate that the preferred or average conformation of *sym*-oxepin oxide (**1**) is significantly flatter than the transoid conformation **1a**. The specific generation of *sym*-2,7-dideuteriooxepin oxide (**9**) from the dideuterioazo compound **8** has provided a means to study the equilibrium subsequently established between **9** and its Cope rearrangement product *sym*-4,5-dideuteriooxepin oxide (**10**). Activation parameters have been obtained for the nitrogen extrusion reactions, **8** → **9** and **8** → **10**, and for the Cope rearrangement, **9** ⇌ **10**.

The structural similarity of *sym*-oxepin oxide² (**1**) (4,8-dioxabicyclo[5.1.0]octa-2,5-diene) to the hydrocarbon homotropilidene (**2**) (bicyclo[5.1.0]octa-2,5-diene) and to the

half oxygenated analogues, the *sym*-oxabicyclo[5.1.0]octa-2,5-dienes (**3**), raises questions about the conformation and possible fluxional structure of **1**. Results obtained by Heil-

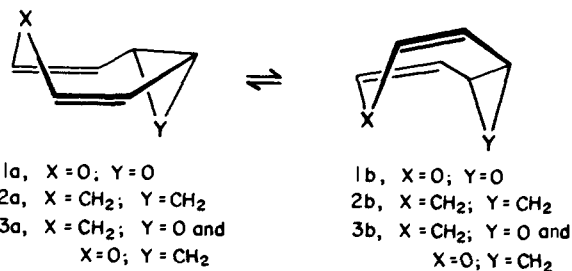


Figure 1. The transoid conformation (1a–3a) and the cisoid conformation (1b–3b) for the related bicyclo[5.1.0]octa-2,5-dienes 1–3.

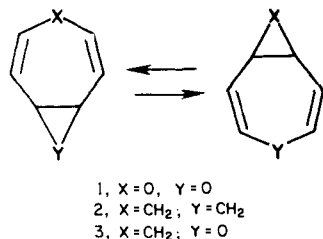


Figure 2. The Cope rearrangements for the related bicyclo[5.1.0]octa-2,5-dienes.

bronner et al.³ from photoelectron spectroscopy indicate a preference for the transoid conformation, **2a**, in homotropilidene (**2**), while analysis of ¹H NMR coupling constants by Grimme et al.⁴ suggests that both equilibrium components of **3** are in the transoid conformations, **3a** (Figure 1). The rapid degenerate Cope rearrangement of **2**⁵ (Figure 2) provided the first example of the utility of ¹H NMR spectroscopy in the detection of such fluxional systems. Subsequently, the ¹H NMR study of the *sym*-oxabicyclo[5.1.0]octa-2,5-dienes (**3**) has shown that an analogous Cope rearrangement interconverts the two valence tautomers,⁴ though at a slower rate than in the hydrocarbon **2**.

In the present work, proton magnetic resonance studies have provided insight into both the conformation and potential Cope rearrangement of the *sym*-oxepin oxide system. Specifically, conformation-dependent proton–proton coupling constants, derived from a computer simulation of the high-resolution ¹H NMR spectrum of *sym*-oxepin oxide (**1**), have been related to possible geometries. While variable temperature studies² failed to show ¹H NMR evidence for the possible degenerate Cope rearrangement of **1**, due to the thermal instability of the molecule, an isotopic labeling study has confirmed the existence of the Cope process for the *sym*-oxepin oxide system by the interconversion of the valence tautomers *sym*-2,7-dideuteriooxepin oxide (**9**) and *sym*-4,5-dideuteriooxepin oxide (**10**). In addition, activation parameters for the Cope rearrangement have been obtained by a variable temperature study.

Spectral Simulation. Method. The 100-MHz proton magnetic resonance spectrum of *sym*-oxepin oxide (**1**) was recorded on a Varian HA-100 spectrometer in deoxygenated CDCl₃ solution, utilizing internal Me₄Si as reference and lock. The spectrum was taken in the frequency sweep mode, at a sweep rate of 1 Hz/100 s, in the direction of decreasing frequency. Appearing in the lower portion of Figure 3 are the three multiplets so observed. Line widths in the spectrum are in the range 0.1–0.2 Hz (width at half-height); some sweep phenomena, e.g., ringing, can still be noted despite the slow sweep rate.

Coupling constants and chemical shifts were determined by least-squares iterative fit using the LAOCN3 method.⁶ Plots of the simulated spectrum by the SIMEQ program⁷ appear in the upper portion of Figure 3.

Results and Discussion

The proton–proton coupling constants obtained from the LAOCN3 iterative simulation are listed in Figure 4. Consid-

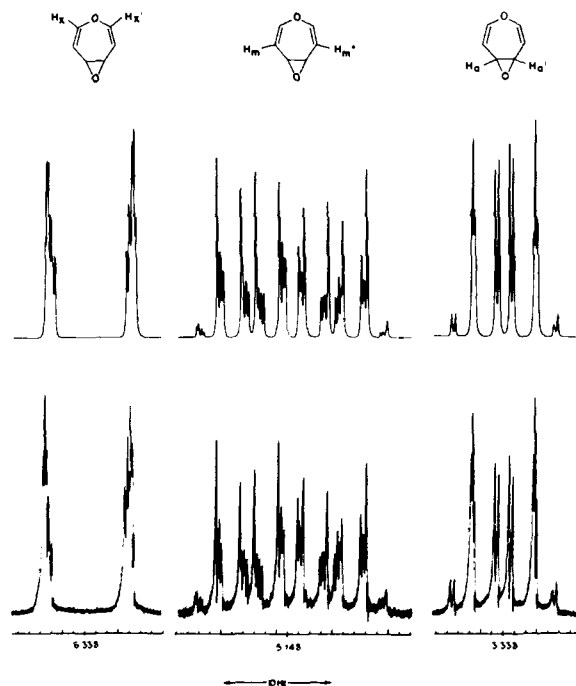


Figure 3. Top: simulated spectrum of *sym*-oxepin oxide (**1**). Plots are by the SIMEQ program⁷ from data derived by the LAOCN3 method.⁶ Bottom: frequency sweep 100-MHz ¹H NMR spectrum of *sym*-oxepin oxide (**1**). Chemical shifts are downfield relative to internal Me₄Si. The direction of sweep was toward decreasing frequency, i.e., from left to right; the rate of sweep was 1 Hz/100 s.

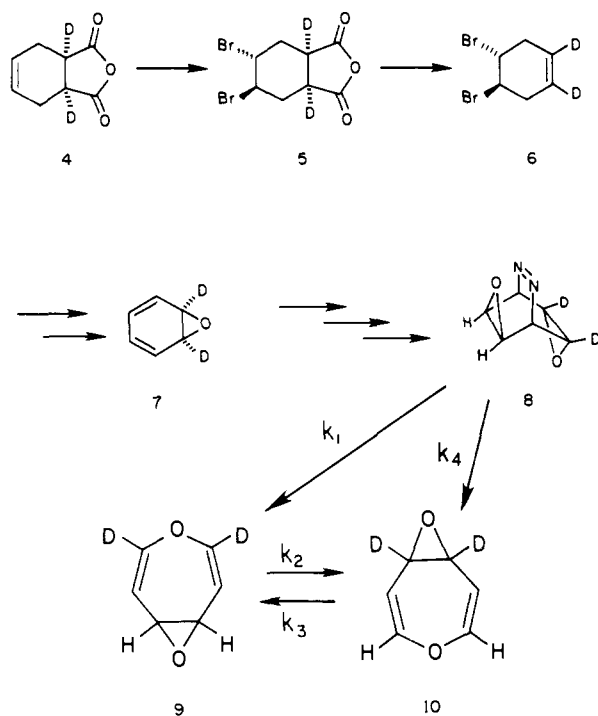
| coupling | coupling constant |
|---------------------|-------------------|
| $J_{aa'}$ | +3.95 Hz |
| $J_{am} = J_{a'm'}$ | +4.52 Hz |
| $J_{ax} = J_{a'x'}$ | +0.42 Hz |
| $J_{am'} = J_{a'm}$ | +1.08 Hz |
| $J_{ax'} = J_{a'x}$ | −0.10 Hz |
| $J_{mm'}$ | +0.06 Hz |
| $J_{mx} = J_{m'x'}$ | +7.44 Hz |
| $J_{m'x} = J_{mx'}$ | +0.40 Hz |
| $J_{xx'}$ | +0.22 Hz |

Figure 4. Coupling constants for *sym*-oxepin oxide (**1**) from the LAOCN3 iterative simulation. Relative positions of the ¹H NMR spectral lines within each multiplet (Figure 3, bottom) were measured to within 0.1 Hz; the error in the tabulated coupling constants simultaneously determined by the positions of several spectral lines is ≤ 0.1 Hz.

eration of molecular models indicates that the sign and/or the magnitude of several of the coupling constants should be sensitive to molecular conformation. In passing from the transoid (**1a**) to the cisoid (**1b**) conformation, the dihedral angle between the vinyl and allylic C–H bonds closes up, becomes zero as the vinyl and allylic C–H bonds eclipse, and then reopens as the molecule adopts the cisoid conformation. Various steric and electronic factors determine the energy profile for the ring inversion **1a** \rightleftharpoons **1b**, and it should not be assumed a priori that the energy minimum need lie at either extreme. The preferred or average conformation might correspond to a more or less flattened geometry between **1a** and **1b**.

Of primary interest in a conformational analysis is the three-bond vinyl–allylic coupling constant, J_{am} ($J_{am} = J_{a'm'}$ = 4.52 Hz). Estimates of the size of the dihedral angle between

Scheme I



the vinyl and allylic C–H bonds can be obtained from the magnitude of J_{am} using the equations of Karplus,⁸ Günther,⁹ and Garbisch.¹⁰ For the two extremes of geometry available to *sym*-oxepin oxide (**1**) the dihedral angles measured¹¹ according to Karplus or Günther are transoid conformation (**1a**), $\phi = 65^\circ$; cisoid conformation (**1b**), $\phi = 16^\circ$. The dihedral angle used by Garbisch for vinyl-allylic systems is measured using a slightly different projection from that used by Karplus and Günther. For **1** the dihedral angles measured¹¹ according to Garbisch are transoid conformation (**1a**), $\phi_{\text{Garbisch}} = 83^\circ$; cisoid conformation (**1b**), $\phi_{\text{Garbisch}} = 23^\circ$.

The calculated geometries for *sym*-oxepin oxide (**1**) based on the equations of Karplus, Günther, and Garbisch are significantly flattened from the geometry of the transoid conformation: Karplus, $\phi = 41^\circ$; Günther, $\phi = 39^\circ$; Garbisch, $\phi_{\text{Garbisch}} = 46^\circ$. Consideration of other factors influencing the size of J_{am} ¹² would most probably *reduce* these estimates of the size of the dihedral angle. Of particular importance is the expected effect of an electronegative substituent (the epoxide oxygen) upon the magnitude of J_{am} ; vicinal coupling to epoxide protons¹³ is significantly smaller than that predicted for an unperturbed ethylenic fragment.

A second coupling constant expected to be conformation dependent is the four-bond vinyl-allylic coupling constant, J_{ax} ($J_{ax} = J_{ax'} = +0.42$ Hz). The sign of J_{ax} is of importance in conformational analysis.^{10,14} For coupling through small dihedral angles the expected sign of J_{ax} is positive; for coupling through large dihedral angles the expected sign is negative. We were unable to simulate the ¹H NMR spectrum of *sym*-oxepin oxide (**1**) adequately using a *negative* sign for J_{ax} . The need for a *positive* sign for J_{ax} in the simulation and the expected dependence of the sign of J_{ax} on the dihedral angle corroborate the conclusion reached with regard to conformation based on the magnitude of J_{am} .

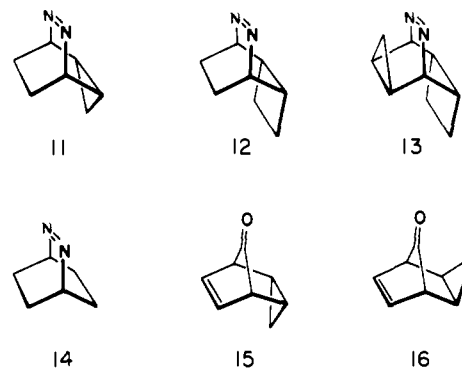
Certainly, only a rough estimate of molecular conformation can be made by the method at hand; yet, analysis of the ¹H NMR spectrum of *sym*-oxepin oxide (**1**) strongly indicates that geometries other than the transoid conformation contribute significantly to the observed three- and four-bond vinyl-allylic coupling constants. Unfortunately, the data do not distinguish among a large variety of possible molecular geometries. Some flattening of the molecule is expected, but the sign and mag-

nitude of J_{am} and J_{ax} are compatible with a range of geometries from flattened transoid (e.g., $\phi \approx 40^\circ$, vide supra) through to the cisoid conformation.

Cope Rearrangement. Strategy. Exchange broadening of the ¹H NMR spectrum of **1** was not observed at temperatures up to 116 °C;² hence, a method *independent of the ¹H NMR time scale* was sought to detect the possible Cope rearrangement in the *sym*-oxepin oxide system. The specific generation of *sym*-2,7-dideuteriooxepin oxide (**9**) or of *sym*-4,5-dideuteriooxepin oxide (**10**) would provide a means to detect the Cope rearrangement via the scrambling of the deuterium labels, **9** \rightleftharpoons **10** (Scheme I). The labeling experiment would not rely on the observation of fluxional behavior of the ¹H NMR spectrum and, thus, could detect a Cope rearrangement proceeding at a rate much slower than that measured for the analogues **2** and **3**.

The specific generation of **9** seemed possible through a modification of the route to *sym*-oxepin oxide (**1**) which would give the dideuterioazo compound **8**. The stereochemistry of the protio analogue of **8** follows unequivocally from its ¹H NMR spectrum;² the structure is that having one epoxide syn and the other anti to the azo bridge. The different orientations of the epoxides in the azo precursor **8** promised the means for the specific generation of the *sym*-dideuteriooxepin oxide **9**.

Considerable attention has been directed toward the study of the participation of small rings in retrograde homo-Diels-Alder reactions. In particular, many examples show striking rate accelerations for the retrograde homo-Diels-Alder reaction for compounds in which the "dienophile" departs anti to the methylene group of an assisting cyclopropane. In the series of azo compounds **11**–**14**¹⁵ the relative rates for nitrogen extrusion show impressively the efficiency of participation by the anti-fused cyclopropane (**11**) and the apparent lack of participation by the syn-fused cyclopropane (**13**): **11**, $k_{\text{rel}} = 1.1 \times 10^{17}$; **12**, $k_{\text{rel}} = 6.7 \times 10^4$; **13**, $k_{\text{rel}} = 8.8 \times 10^2$; **14**, $k_{\text{rel}} = 1.0$.



Similarly, for the bridged ketones **15** and **16**¹⁶ the participation of the anti-fused cyclopropane (**15**) in the extrusion of carbon monoxide leads to a marked difference in the thermal stability of the two compounds: **15**, $t_{1/2}^{35.0^\circ\text{C}} = 89$ min; **16**, $t_{1/2}^{150.0^\circ\text{C}} = 82$ min.

The specific geometric requirement for effective cyclopropyl participation in the retrograde homo-Diels-Alder reaction was used in a stereospecific conversion of 1,3- to 1,4-dienes by Berson and Olin.¹⁷ Using a series of azo compounds they showed that in the retrograde homo-Diels-Alder reaction strong preference is manifest for a transition state in which nitrogen departs anti to the methylene group of the cyclopropane ring, even when the alternate transition state allowing syn departure of nitrogen is conformationally accessible and sterically favored.

The participation of the cyclopropane ring in nitrogen extrusion reactions is envisioned by Jorgensen¹⁸ to occur through the mixing of the e_s type orbital of the cyclopropane with the unoccupied σ^*_{CN} orbitals between carbon and departing ni-

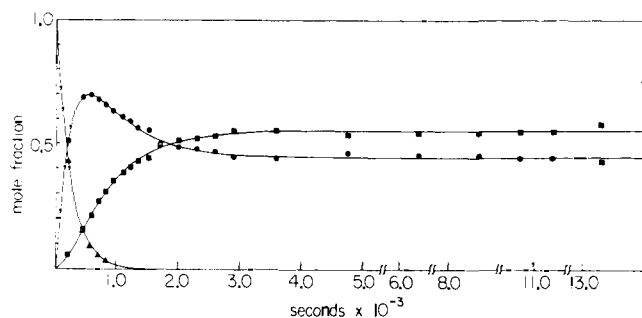


Figure 5. The mole fractions measured for **8** (\blacktriangle), **9** (\bullet), and **10** (\blacksquare), and the curves predicted from eq 4–6 using the nonlinear least-squares parameters from Table I, for the kinetic run at 39.8 °C.

trogen. The overlap of the e_s and σ^*_{CN} orbitals is expected to be markedly reduced for cases where the cyclopropane is syn fused to the azo linkage; the participation of the cyclopropane is predicted and observed to be correspondingly reduced.

Ample precedent thus indicated that the anti-fused epoxide of the dideuterioazo compound **8** would participate in a nitrogen extrusion reaction ($k_1 \gg k_4$, Scheme I), selectively generating *sym*-2,7-dideuteriooxepin oxide (**9**). By dissolution of **8** in DCCl_3 at ambient temperatures² we expected to observe loss of nitrogen (**8** \rightarrow **9**) followed by the establishment of the equilibrium **9** \rightleftharpoons **10**, now, due to isotopic labeling, no longer a degenerate Cope rearrangement. From the lack of exchange broadening of the ^1H NMR spectrum of **1** at 116 °C² we expected the rate of the Cope rearrangement (k_2 and k_3 , Scheme I) to be slower than, or comparable to, the rate for nitrogen extrusion² (k_1 , Scheme I), thereby allowing these three rate constants to be measured.

Synthetic Approach. Ideally, the chemistry developed for the synthesis of *sym*-oxepin oxide² (**1**) could be used in the synthesis of the dideuterioazo compound **8** with only minor variations. The needed starting material for application of the *sym*-oxepin oxide synthesis to the synthesis of the *sym*-dideuterio analogue(s) is 1,2-dideuteriobenzene oxide (**7**). By analogy to the benzene oxide synthesis,¹⁹ **7**, in turn, could be obtained from 1,2-dideuterio-*trans*-4,5-dibromocyclohexene (**6**). The task at hand was the expeditious production of **6**. The route adopted (Scheme I) contained one step for which the analogous protio transformation was unknown, the oxidative cleavage of anhydride **5** to the desired olefin **6**. The transformation was achieved, albeit in low yield (3%), by the action of $\text{Pb}(\text{OAc})_4$ in pyridine directly on the anhydride **5**. Despite the low yield, the purification of **6** is not tedious and is efficiently accomplished by chromatography over silica gel (see Experimental Section). Thus, the route to the azo compound **8** begins with the formation of the adduct **4**²⁰ of dideuteriomaleic anhydride²¹ and butadiene; **4** is brominated according to the procedure for the protio material²² and the product **5** transformed to the dideuterioazo compound **8** by the sequence outlined in Scheme I.

Method. The dideuterioazo compound **8** was liberated from its cuprous complex² at -20 °C and was isolated as a white

crystalline solid by low-temperature evaporation of its methylene chloride solution. Rapidly prepared solutions of **8** in DCCl_3 were stored at -78 °C until their use in the kinetic runs. The kinetics were done in a Varian XL-100 temperature regulated probe at temperatures between ca. 15 and 40 °C.²³ The progress of the reactions (k_1 , k_2 , k_3 , and k_4 , Scheme I) was monitored by Fourier transform ^1H NMR spectroscopy, using spectral parameters selected to allow accurate integration of the proton absorptions in **8**, **9**, and **10**. The spectra were stored on magnetic tape prior to plotting and integration to allow rapid accumulation of data at the higher temperatures.

The kinetic expressions for nitrogen extrusion from **8** and for the subsequent Cope rearrangement can be written (cf. Scheme I)

$$d[\mathbf{8}]/dt = -k_1[\mathbf{8}] - k_4[\mathbf{8}] \quad (1)$$

$$d[\mathbf{9}]/dt = k_1[\mathbf{8}] - k_2[\mathbf{9}] + k_3[\mathbf{10}] \quad (2)$$

$$d[\mathbf{10}]/dt = k_2[\mathbf{9}] - k_3[\mathbf{10}] + k_4[\mathbf{8}] \quad (3)$$

Expressing the concentrations of **8**, **9**, and **10** as mole fractions, the rate expressions can be solved giving eq 4–6.²⁴

$$[\mathbf{8}] = e^{-(k_1+k_4)(t-t_0)} \quad (4)$$

$$[\mathbf{9}] = \left\{ \frac{k_3}{k_2 + k_3} \right\} [1 - e^{-(k_2+k_3)(t-t_0)}] + \left\{ \frac{(k_1 - k_3)}{(-k_1 + k_2 + k_3 - k_4)} \right\} \times [e^{-(k_1+k_4)(t-t_0)} - e^{-(k_2+k_3)(t-t_0)}] \quad (5)$$

$$[\mathbf{10}] = 1 - [\mathbf{8}] - [\mathbf{9}] \quad (6)$$

In eq 4 and 5, time = t ; t_0 , a parameter to be determined, is the time at which $[\mathbf{8}] = 1$ and $[\mathbf{9}] = [\mathbf{10}] = 0$.²⁵ The data for $[\mathbf{8}]$, $[\mathbf{9}]$, and $[\mathbf{10}]$ from the kinetic runs at each temperature were fitted for the best values of k_1 , k_2 , k_3 , k_4 , and t_0 using nonlinear least-squares techniques.

Results

The retrograde homo-Diels–Alder reaction (k_1 and k_4 , Scheme I) and the subsequent Cope rearrangement (k_2 and k_3 , Scheme I) display the general behavior shown for the 39.8 °C run in Figure 5. For all kinetic runs, a close match is seen between the experimental concentrations of **8**, **9**, and **10** and the concentrations predicted from eq 4–6 using the parameters k_1 , k_2 , k_3 , k_4 , and t_0 derived by nonlinear least-squares fitting. The deviations of the measured concentrations from the calculated concentrations are well within the limits of error expected from the integration of ^1H NMR spectrum absorptions (ca. 5%) and show the measured concentrations to be compatible with the kinetic behavior described by eq 4–6. The parameters for all of the kinetic runs, derived by nonlinear least-squares fitting of the measured concentrations to eq 4–6, are listed in Table I.

The dependence of each rate constant on temperature (Table I) was used to determine the parameters for the Arrhenius equation, $k_x = Ae^{-E_a/RT}$ ($x = 1, 2, 3$, and 4). The values for A and E_a , in turn, were used to calculate the enthalpy (ΔH^\ddagger) and the entropy (ΔS^\ddagger) of activation, through the use of ab-

Table I. Nonlinear Least-Squares Parameters and Experimental Conditions for the Kinetic Runs for the Reaction Sequence $\mathbf{8} \rightarrow \mathbf{9} \rightleftharpoons \mathbf{10}$ (See Scheme I)^a

| Temp, °C ^b | $k_1 \times 10^5, \text{s}^{-1}$ | $k_2 \times 10^5, \text{s}^{-1}$ | $k_3 \times 10^5, \text{s}^{-1}$ | $k_4 \times 10^5, \text{s}^{-1}$ | t_0, s^c | Longest t obsd, s | No. of spectral integrations |
|-----------------------|----------------------------------|----------------------------------|----------------------------------|----------------------------------|-------------------|---------------------|------------------------------|
| 39.8 | 415 \pm 12 | 78.3 \pm 2.2 | 62.6 \pm 2.1 | 7.3 \pm 4.8 | +42 \pm 8 | 13 350 | 49 |
| 30.0 | 96.1 \pm 1.3 | 22.6 \pm 0.6 | 18.0 \pm 0.6 | 0.36 \pm 0.75 | +27 \pm 12 | 25 920 | 44 |
| 19.9 | 22.1 \pm 0.2 | 6.70 \pm 0.12 | 5.20 \pm 0.15 | 0.52 \pm 0.12 | -62 \pm 15 | 32 400 | 48 |
| 14.8 | 10.2 \pm 0.1 | 3.13 \pm 0.08 | 2.23 \pm 0.12 | 0.03 \pm 0.06 | -105 \pm 33 | 48 960 | 78 |

^a Error limits are standard deviations. ^b See ref 23. ^c See ref 25.

solute reaction rate theory.²⁶ The activation parameters are tabulated (Table II).

Discussion

From the rate constant values and error estimates in Table I, the magnitude of k_4 is calculated to be less than $k_1/25$ at the 95% confidence limit. The values for k_4 , however, are at the lower limit of sensitivity of our method of measurement (see error limits in Table I); the magnitude of k_4 may be much smaller. The observed values of the ratio k_1/k_4 indicate that the nitrogen extrusion occurs almost entirely by the process $8 \rightarrow 9$ (k_1).

Other representative aspects of the kinetic system are revealed by the concentration curves for **8**, **9**, and **10** at 39.8 °C (Figure 5). Initially, the first-order decomposition of the azo compound **8** ($k_1 \gg k_4$) to the dideuteroioxepin oxide **9** leads to a sharp rise in the concentration of the latter species to a value well above that attained at equilibrium. The equilibrium $9 \rightleftharpoons 10$, at 39.8 °C, reaches the steady state ($[9] = 0.44$ mole fraction, $[10] = 0.56$ mole fraction) after ca. 5000 s, with an equilibrium constant, $K_{eq}^{39.8^\circ C} = k_2/k_3 = 1.25$, corresponding to a thermodynamic, secondary isotope effect of 1.12 per C–D bond. The magnitude of the isotope effect is similar to the value of 1.09 per C–D bond, at the same temperature, calculated for the Cope process, biallyl-1,1,6,6-*d*₄ \rightleftharpoons biallyl-3,3,4,4-*d*₄.²⁷ As with the biallyl system, the equilibrium between the *sym*-dideuteroioxepin oxides **9** and **10** lies to the side of the species bearing the deuterium atoms adjacent to the C–C bond broken in the Cope rearrangement. In the process $10 \rightarrow 9$ the breaking of the epoxide C–C bond is expected to be slowed by the deuterium substitution, while a small acceleration for epoxide C–C bond formation is expected in the reverse process, $9 \rightarrow 10$.²⁷

The activation parameters listed in Table II are of particular interest when compared to parameters found for compounds similar in structure to the azo compound **8** or to the *sym*-dideuteroioxepin oxides **9** and **10**. The activation parameters for the loss of nitrogen from the azo compounds **11**–**14** have been reported:^{15,28} **11**, $E_a = 14.9 \pm 1.5$ kcal/mol, $\Delta S^\ddagger = -21$ eu; **12**, $E_a = 39.2 \pm 0.3$ kcal/mol, $\Delta S^\ddagger = +11$ eu; **13**, $E_a = 41.4 \pm 0.3$ kcal/mol, $\Delta S^\ddagger = +10.3$ eu; **14**, $E_a = 44.6 \pm 0.2$ kcal/mol, $\Delta S^\ddagger = +10.5 \pm 0.3$ eu. In **11** and in similar azo compounds²⁹ believed to decompose in a concerted fashion with a high degree of cyclopropyl participation, the energies of activation are relatively low, indicating a release of small ring strain in the respective transition states. Further, the entropies of activation are negative, despite the dissociative nature of the reactions, indicative of transition states more highly ordered than the respective reactant ground-state configurations. High bond order and low diradical character are expected in the transition states for these concerted reactions. In **12**–**14** decreased bent bond character and/or geometrical restraints on small ring participation lead to an expected decrease or curtailment of bond-breaking concert, and, correspondingly, the activation energies are relatively high and the entropies of activation positive. For **12** the overlap between the small ring and the two breaking C–N bond orbitals has become sufficiently small that a diradical coupling product is seen in addition to the cycloreversion product.³⁰ Yet, in two 3,4-diazabicyclo[4.2.0]octenes studied by Berson et al.,³¹ the rates for nitrogen extrusion are only slightly larger than that for **12** (a factor of ca. 5) but discrete diradical intermediates can be ruled out from the stereospecificity of product formation and the lack of diradical coupling products; the reactions here, as for **11**, must be called “concerted”.

The term “concerted” seemingly applies to a broad range of nitrogen extrusion reactions showing a wide variation in the degree of transition state small-ring participation. The acti-

Table II. Activation Parameters for the Nitrogen Extrusion Reactions ($8 \rightarrow 9$ and $8 \rightarrow 10$) and for the Forward ($9 \rightarrow 10$) and Reverse ($10 \rightarrow 9$) Cope Rearrangements^a

| Reaction | Log A | E_a , kcal/mol | $\Delta H^\ddagger_{300\text{ K}}$, kcal/mol | $\Delta S^\ddagger_{300\text{ K}}$, eu |
|--------------------------|--------------|------------------|---|---|
| $8 \xrightarrow{k_1} 9$ | 16.12 ± 0.32 | 26.5 ± 0.4 | 25.9 ± 0.4 | +13.2 ± 1.5 |
| $9 \xrightarrow{k_2} 10$ | 12.81 ± 0.33 | 22.8 ± 0.4 | 22.2 ± 0.4 | -1.9 ± 1.5 |
| $10 \xrightarrow{k_3} 9$ | 13.23 ± 0.47 | 23.5 ± 0.6 | 22.9 ± 0.6 | 0.0 ± 2.2 |
| $8 \xrightarrow{k_4} 10$ | 18.77 ± 8.56 | 33.0 ± 11.7 | 32.4 ± 11.7 | +25.4 ± 39.2 |

^a Error limits are standard deviations. The large relative errors in the values of k_4 (see Table I) cause imprecise determination of the activation parameters for the process $8 \xrightarrow{k_4} 10$.

vation energy gap between the concerted and the nonconcerted (diradical) mechanisms may become small when factors which decrease the overlap between the small ring and the orbitals in the breaking azo C–N bonds lead to a decreased participation by the small ring. While the large-rate acceleration for nitrogen extrusion from **11** (*vide supra*) must be attributed to a large degree of cyclopropane C–C bond breaking in the transition state, a much smaller degree of small ring C–C bond breaking in the transition state could account for the stereospecificities in the cycloreversions of the 3,4-diazabicyclo[4.2.0]octenes studied by Berson et al. or could account for the preferred opening of the anti-fused epoxide of the deuterioazo compound **8**. Clearly, product distribution is not a sensitive indicator of the degree of concert during cycloreversion; the activation energy gap between concerted and diradical mechanisms need not be large for the diradical derived products to drop below the levels of detection.

The energy of activation for the process $8 \rightarrow 9$ seems to reflect some release of strain in the transition state (cf. **11** and **14**). That a portion of the strain is released by some anti-fused epoxide C–C bond breaking in **8** is indicated by the predominant formation of **9** in the retrograde homo-Diels–Alder reaction. The high ΔS^\ddagger suggests, however, less concert (more diradical character) in the conversion $8 \rightarrow 9$ than in nitrogen extrusion from **11**, due, presumably, to a less efficient overlap in **8** of the anti-fused, small-ring, bent C–C bond with the orbitals of the two breaking C–N bonds. The reduction in overlap can be expected from the shapes of the molecular orbitals in cyclopropane and oxirane³² and has been used by Grimme³³ to explain the differences in small-ring participation in the Cope rearrangement. The similar rates for nitrogen extrusion from **8** ($k_1^{30.0^\circ C} + k_4^{30.0^\circ C} = 9.65 \pm 0.15 \times 10^{-4} \text{ s}^{-1}$) and from its protio analogue² ($k^{29.8^\circ C} = 9.51 \pm 0.15 \times 10^{-4} \text{ s}^{-1}$) suggest that, at most, a small, kinetic, secondary isotope effect exists for the nitrogen extrusion.³⁴ A small, secondary isotope effect would corroborate the finding based on ΔS^\ddagger that only a small amount of epoxide C–C bond breaking has occurred in the transition state for $8 \rightarrow 9$.

The kinetic data for the process $9 \rightleftharpoons 10$ support the finding that the rates for Cope rearrangement follow the order $2 > 3 > 1$.^{2,33} The free energies of activation calculated for the three processes reflect the rate differences: **2**, $\Delta G^\ddagger = 14.6 \pm 0.2$ kcal/mol;^{35,36} **3**, $\Delta G^\ddagger \approx 17$ kcal/mol;^{4,37} $9 \rightarrow 10$, $\Delta G^\ddagger = 22.8 \pm 0.6$ kcal/mol.³⁶

The principal contributor to the high ΔG^\ddagger for the conversion $9 \rightarrow 10$ is ΔH^\ddagger (Table II). The magnitude of ΔH^\ddagger for the process $9 \rightarrow 10$ can be attributed to the reduced bent bond character expected for the epoxides³² of **9** and **10** (cf. the cyclopropanes of **2** and **3**). For Cope rearrangements in the series **2**, **3**, and **9**, bent bond character in the cyclopropane or epoxide C–C bonds will enhance the orbital overlaps required in the bond-breaking and bond-making steps leading from ground states to transition states. Stated more simply, π character in

the small ring C-C bonds of **2**, **3**, and **9** will enhance cyclic bishomoconjugation in the Cope transition states. Hence, in the series **2**, **3**, and **9**, decreasing bent bond character in the small ring ground states and the corresponding decrease of cyclic bishomoconjugation in the respective transition states may account for the observed trend of ΔG^{\ddagger} 's.

Interestingly, the entropy of activation for the Cope process in homotropilidene (**2**), determined by line-shape analysis of the fluxional ^1H NMR spectrum of the d_8 analogues,³⁵ is -8.0 ± 0.3 eu, a value noticeably more negative than the -1.9 ± 1.5 eu for the process **9** \rightarrow **10**. Comparison of these figures, and of the errors inherent in their measurement, indicates that the ΔS^{\ddagger} for *sym*-oxepin oxide (**1**) is less negative than that for homotropilidene (**2**). The less negative ΔS^{\ddagger} for the process **9** \rightarrow **10** may be attributed to a transition state for Cope rearrangement of **9** having less stringent geometrical constraints than those existing during Cope rearrangement of **2**. In particular, cyclic bishomoconjugation in the transition state for **9** is expected to be less efficient than for **2** (vide supra). Consequently, deviations away from the geometry of optimal bishomoconjugation will raise the E_a for Cope rearrangement of **9** less than similar deviations would raise the E_a for Cope rearrangement of **2**.³⁸ A lower ΔH^{\ddagger} for **2** is achieved only at the expense of a more geometrically constrained transition state (more negative ΔS^{\ddagger}).

As ΔS^{\ddagger} reflects differences in ground-state and transition-state entropies, the ΔS^{\ddagger} for the process **9** \rightarrow **10** may also reflect a more constrained ground state in **9** than in **2**. The presumed, flattened conformation (vide supra) for **9** may be less conformationally mobile, i.e., more rigid, than the ground-state conformation for **2**.³

Experimental Section

^1H NMR spectra (100 MHz) were obtained on a Varian HA-100 or Varian XL-100 spectrometer. For all deuterated compounds the percent deuteration and the chemical shifts (downfield from internal Me_4Si) for the residual protons at the positions of deuteration are reported; otherwise the ^1H NMR spectra were identical with the spectra of the undeuterated analogues. Mass spectra were determined on an AEI MS-9 double-focusing, high-resolution, mass spectrometer and infrared spectra on a Perkin-Elmer 137 spectrometer. Melting points are uncorrected and were obtained on a Kofler hot stage.

sym-Oxepin oxide (1) for use in the high-resolution ^1H NMR studies was prepared using the method previously described.^{2,39} A sample of the azo precursor² prepared from its cuprous complex (186.8 mg, approximately 0.7 mmol) was allowed to stand at ambient temperature in CDCl_3 - Me_4Si (basic alumina treated) solution until virtually complete conversion to *sym*-oxepin oxide (**1**) had occurred (1.75 h, monitored by ^1H NMR). The CDCl_3 - Me_4Si solution of **1** was vacuum transferred at ambient temperature and 0.02 mmHg, thoroughly degassed by freeze-thaw techniques, and sealed in a ^1H NMR sample tube under nitrogen; the final solution volume was approximately 0.3 ml.

Deuteration Sequence. For each compound the literature method for its preparation or for the preparation of its undeuterated analogue is referenced.

Dideuteriomaleic anhydride²¹ used as starting material was 92% deuterated, as determined by ^1H NMR using an internal reference.

cis-1,2-Dideuterio-3,6-dihydrophthalic anhydride (4)²⁰ was 93% deuterated, as determined by the residual ^1H NMR absorption at δ 3.43 (CDCl_3).

cis-1,2-Dideuterio-trans-4,5-dibromocyclohexanedicarboxylic acid anhydride (5)²² was 93% deuterated, as determined by the residual absorption at δ 3.66 (acetone- d_6): mass spectrum (70 eV) small parent two Br triplet, m/e 312, 314, 316; ir (KBr) 1850, 1780, 945 cm^{-1} ; mp 134–136 $^{\circ}\text{C}$.

1,2-Dideuterio-trans-4,5-dibromocyclohexene (6).⁴⁰ The oxidative cleavage of **5** by $\text{Pb}(\text{OAc})_4$ was carried out in a four-neck reaction vessel connected to a vacuum manifold, equipped with a thermometer and a mechanical stirrer, and attached by means of Gooch tubing to a vessel containing $\text{Pb}(\text{OAc})_4$. To **5** (5.96 g, 19.0 mmol) was added

dry pyridine (240 ml); the mixture was partially frozen (liquid nitrogen bath); then the system was evacuated [including the $\text{Pb}(\text{OAc})_4$ vessel by a separate connection to the vacuum manifold]. After thawing, but while still cold, the stirred pyridine solution was degassed by cycles of evacuation and filling of the system with argon. Under an argon atmosphere $\text{Pb}(\text{OAc})_4$ (Matheson Coleman and Bell) (34.08 g, 77.0 mmol) was added in one portion through the Gooch tubing to the cold (-19 $^{\circ}\text{C}$) pyridine solution. The stirred heterogeneous mixture was heated by application of an oil bath at 54 $^{\circ}\text{C}$. Once the internal temperature had reached 47 $^{\circ}\text{C}$ (17 min of heating) the orange heterogeneous reaction mixture became homogeneous with the concurrent, vigorous evolution of gas. The oil bath heating of the reaction was continued for an additional 5 min during which time the internal temperature rose to 52 $^{\circ}\text{C}$ and the mixture turned deep brown. The oil bath was removed and a liquid nitrogen cooling bath was applied until the internal temperature dropped below -20 $^{\circ}\text{C}$.

The cold reaction was quenched by pouring the mixture into cold 37% aqueous HCl (240 ml) plus crushed ice (500 cc). The resulting suspension was thoroughly extracted with Et_2O and the organic layers were pressure filtered through sintered glass to remove the suspended solids. The filtered extracts were combined and washed with 1 N HCl and then with saturated, aqueous NaHCO_3 . Drying of the organic layer (MgSO_4) and removal of the Et_2O by distillation (Vigreux column) gave a tan, oily solid which was chromatographed over activity III silica gel (75 g) (CH_2Cl_2 eluent). The dibromo olefin **6** was completely eluted by less than 200 ml of CH_2Cl_2 and was obtained by evaporation (Vigreux column) of the eluent; the yield was 143.3 mg (3%) of **6**. The ^1H NMR spectra of **6** show a loss of deuterium content during the oxidative cleavage; the residual proton absorptions at δ 5.65 (CDCl_3), in spectra from several reactions, indicate a deuterium content ranging from 72 to 82%. The chromatographed dibromo olefin **6** was used without further purification in the subsequent epoxidation to give 1,2-dideuterio-*trans*-4,5-dibromocyclohexene oxide.

1,2-Dideuterio benzene Oxide (7).^{2,19,39} 1,2-Dideuterio-*trans*-4,5-dibromocyclohexene oxide produced by epoxidation^{41,42} of dibromo olefin **6** was 77% deuterated, as determined by the residual ^1H NMR absorption at δ 3.23 (CDCl_3); mass spectrum (70 eV) small parent two Br triplet, m/e 256, 258, 260; ir (CHCl_3) 2200, 1170, 900 cm^{-1} .

Dehydrobromination^{2,19} gave **7** which was 74% deuterated, as determined by the residual ^1H NMR absorption at δ 5.07 (CDCl_3).

Dideuterioazodiepoxide 8.² The adduct² of dideuterio benzene oxide **7** with bis(trichloroethyl)azodicarboxylate was 77% deuterated, as determined by the residual ^1H NMR absorptions at δ 3.78 and 3.56 (CDCl_3); mass spectrum (70 eV) parent six Cl cluster, m/e 474, 476, 478, 480, 482, 484, 486; ir (KBr) 1760, 1730 cm^{-1} ; mp 143–145 $^{\circ}\text{C}$.

Epoxidation of the dideuterio adduct to give the corresponding diepoxide was achieved by the method described for the protio analogue;² the diepoxide was 76% deuterated, as determined by the residual ^1H NMR absorption at δ 3.72 (CDCl_3); mass spectrum (70 eV) parent six Cl cluster, m/e 490, 492, 494, 496, 498, 500, 502; ir (KBr) 1775, 1725 cm^{-1} ; mp 189.0–190.5 $^{\circ}\text{C}$.

Deprotection and oxidation² gave **8** as its cuprous complex:² ir (KBr) 1465 cm^{-1} .

The dideuterioazodiepoxide **8** was isolated at low temperature by the procedure detailed for the undeuterated material.² The epoxide proton absorptions at δ 3.50 and 3.40 (CDCl_3 , probe temperature -20 $^{\circ}\text{C}$) had intensities in the ratio of 23:100, indicating 77% deuteration of the anti-fused epoxide.

Kinetic Runs. Generation of the Dideuteriooxepin Oxides 9 and 10.³⁹ For each kinetic run, dideuterioazodiepoxide **8** (5.9–7.6 mg, 0.042–0.054 mmol) was rapidly dissolved and transferred to a ^1H NMR sample tube with CDCl_3 (350 μl , basic alumina treated). The sealed sample tube was stored at -78 $^{\circ}\text{C}$ until its use in the kinetic run. To initiate each run, the sample tube was removed from the -78 $^{\circ}\text{C}$ bath and inserted in a Varian XL-100 spectrometer probe pre-equilibrated to the desired temperature.²³ The sample remained in the temperature-regulated probe throughout each run and the progress of the reactions was monitored by Fourier transform pulse spectroscopy. The spectral parameters utilized (16 approximately 45 $^{\circ}$ radiofrequency pulses; acquisition time of 2 s) gave relative peak intensities which were the same obtained in spectra using a 30-s delay between radiofrequency pulses.

The progress of the cycloreversion, **8** \rightarrow **9**, was monitored by the

ratio of the intensity of the bridgehead protons of **8** (δ 6.08) to the intensity of the corresponding protons (at C₃ and C₆) in the *sym*-oxepin oxides (δ 5.14). The progress of the Cope rearrangement, **9** \rightleftharpoons **10**, was monitored by the increase in the intensity of the *sym*-dideuteriooxepin oxide residual proton absorptions at δ 6.33 (protons at C₂ and C₇) relative to the absorption at δ 5.14 (protons at the undeuterated positions, C₃ and C₆), applying the appropriate correction for the percentage of deuteration. The *sym*-oxepin oxides **9** and **10** were 75% deuterated, as determined by the residual proton absorptions at δ 3.33 and 6.33.

Acknowledgments. Special thanks are extended to Professor R. B. Woodward for his generous support and guidance, to Professors M. Karplus and B. D. Sykes for their encouragement and valuable discussions, to Drs. J. M. Fitzpatrick, W. E. Hull, and S. L. Patt for their expert technical assistance, and to Dr. R. W. Burchfield for his help in the analysis of the kinetic data. W.H.R. gratefully acknowledges a National Science Foundation predoctoral fellowship (1972–1975), and partial support from the donors of the Petroleum Research Fund, administered by the American Chemical Society; D.D.H. gratefully acknowledges a National Institutes of Health traineeship (1972–1976).

References and Notes

- Address correspondence to this author at the Department of Chemistry, Massachusetts Institute of Technology, Cambridge, Mass. 02139.
- W. H. Rastetter, *J. Am. Chem. Soc.*, preceding paper in this issue.
- P. Bischof, R. Gleiter, E. Heilbronner, V. Hornung, and G. Schröder, *Helv. Chim. Acta*, **53**, 1645 (1970).
- H. Klein, W. Kursawa, and W. Grimme, *Angew. Chem., Int. Ed. Engl.*, **12**, 580 (1973).
- W. von E. Doering and W. R. Roth, *Angew. Chem., Int. Ed. Engl.*, **2**, 115 (1963).
- A. A. Bothner-By and S. Castellano, Department of Chemistry, Carnegie-Mellon University, Pittsburgh, Pa. 15213.
- C. W. Kort and P. J. van der Haak, Laboratory of Organic Chemistry, Amsterdam University, Amsterdam, The Netherlands.
- M. Karplus, *J. Chem. Phys.*, **30**, 11 (1959).
- H. Günther, H. Klose, and D. Cremer, *Chem. Ber.*, **104**, 3884 (1971).
- E. W. Garbisch, Jr., *J. Am. Chem. Soc.*, **86**, 5561 (1964).
- Dihedral angles measured from Dreiding models; angles expected to be accurate to within 5°.
- L. M. Jackman and S. Sternhell, "Applications of Nuclear Magnetic Resonance Spectroscopy in Organic Chemistry", 2d ed, Pergamon Press, New York, N.Y., 1969, Chapter 4-2.
- (a) K. Tori, T. Komeno, and T. Nakagawa, *J. Org. Chem.*, **29**, 1136 (1964); (b) H.-J. Altenbach and E. Vogel, *Angew. Chem., Int. Ed. Engl.*, **11**, 937 (1972); (c) D. B. Borders and J. E. Lancaster, *J. Org. Chem.*, **39**, 435 (1974).
- H. Günther, *Z. Naturforsch. B*, **24**, 680 (1969).
- E. L. Allred and K. J. Voorhees, *J. Am. Chem. Soc.*, **95**, 620 (1973), and references cited therein.
- B. Halton, M. A. Battiste, R. Rehberg, C. L. Deyrup, and M. E. Brennan, *J. Am. Chem. Soc.*, **89**, 5964 (1967).
- J. A. Berson and S. S. Olin, *J. Am. Chem. Soc.*, **91**, 778 (1969).
- W. L. Jorgensen, *J. Am. Chem. Soc.*, **97**, 3082 (1975).
- E. Vogel and H. Günther, *Angew. Chem., Int. Ed. Engl.*, **6**, 385 (1967).
- (a) D. E. Van Sickle and J. O. Rodin, *J. Am. Chem. Soc.*, **86**, 3091 (1964); (b) A. C. Cope and E. C. Herrick, *ibid.*, **72**, 983 (1950).
- C. Di Lauro, S. Califano, and G. Adembri, *J. Mol. Struct.*, **2**, 173 (1968).
- V. F. Kucherov, A. L. Shabanov, and A. S. Onishchenko, *Bull. Acad. Sci. USSR, Div. Chem. Sci.*, 763 (1963).
- The Varian XL-100 variable temperature accessory is specified to hold temperature constant to within ± 2 °C. The maximum variation recorded between the initial temperature and the temperature upon completion of any kinetic run did not exceed 0.4 °C (temperatures measured by probe thermometer).
- The rate law for **8** (eq 1) depends only on **[8]**; eq 4, hence, represents the unimolecular N₂ extrusion from azo compound **8**. The rate law for **9** (eq 2) can be solved by utilizing the known dependence of **[8]** upon time (eq 4) and the mass balance requirement (eq 6). Substitution of eq 4 and 6 into eq 2 leads to a rate expression for **[9]** involving the concentration of only species **9**:

$$d[9]/dt = (k_1 - k_3)e^{-[(k_1+k_3)t-t_0]} - (k_2 + k_3)[9] + k_3 \quad (7)$$
- Equation 5 is obtained from eq 7 by (a) multiplication of eq 7 by the integration factor $e^{[(k_2+k_3)t-t_0]}$, (b) integration from initial time ($t = t_0$) to observation time, and (c) division of the resultant equation by the factor $e^{[(k_2+k_3)t-t_0]}$.
- The time t is the time elapsed before each observation and is measured from the time of initial warming of the sample. A small correction to t , t_0 , is made to account for (a) time for dissolution of **8** in CDCl₃ prior to cooling to -78 °C, (b) time for sample warming from -78 °C to probe temperature, and (c) time for spectroscopic observation (16 rf pulses at an acquisition time of 2 s).
- See, for example, F. Daniels and R. A. Alberty, "Physical Chemistry", Wiley, New York, N.Y., 1966, p 613.
- K. Humski, R. Malojcic, S. Borcic, and D. E. Sunko, *J. Am. Chem. Soc.*, **92**, 6534 (1970).
- Although the authors do not quote error estimates for the values of ΔS^\ddagger for compounds **11**–**13**, the method of measurement is expected to yield values of ΔS^\ddagger with inherent errors less than 2 eu.
- E. L. Allred and A. L. Johnson, *J. Am. Chem. Soc.*, **93**, 1300 (1971).
- E. L. Allred and J. C. Hinshaw, *Tetrahedron Lett.*, 387 (1972).
- J. A. Berson, E. W. Petrillo, Jr., and P. Bickart, *J. Am. Chem. Soc.*, **96**, 636 (1974).
- W. L. Jorgensen and L. Salem, "The Organic Chemist's Book of Orbitals", Academic Press, New York, N.Y., 1973, pp 154, 160.
- H. Klein and W. Grimme, *Angew. Chem., Int. Ed. Engl.*, **13**, 672 (1974).
- Each rate is determined from a single kinetic run. The difference between 30.0 and 29.8 °C is less than the expected temperature fluctuations during each kinetic run (see ref 23).
- H. Günther, J. B. Pawliczek, J. Ulmen, and W. Grimme, *Angew. Chem., Int. Ed. Engl.*, **11**, 517 (1972).
- Calculated from ΔH^\ddagger and ΔS^\ddagger at 353 K (80 °C), the approximate ¹H NMR spectrum coalescence temperature for compound **3** (see ref 4).
- Although the authors do not quote an error estimate for the value of ΔG^\ddagger for compound **3**, the method of measurement is expected to yield a value of ΔG^\ddagger with an inherent error less than 1 kcal/mol.
- By analogy to the rearrangements of **2**³⁵ and **3**,⁴ the conformation for optimal bishomoconjugation in the Cope rearrangement transition state for *sym*-oxepin oxides is assumed to be the cisoid conformation **1b**.
- All glassware used in the preparation or handling of the *sym*-oxepin oxides, **1**, **9**, and **10**, and of benzene oxide-oxepin (**7**) was base treated.²
- J. P. Wibaut and F. A. Haak, *Recl. Trav. Chim. Pays-Bas*, **67**, 85 (1948).
- G. J. Kasperik and T. C. Bruice, *J. Am. Chem. Soc.*, **94**, 198 (1972).
- We found the 15-h reaction time used for epoxidation by Bruice et al.⁴¹ to be unnecessarily long; epoxidation by *m*-chloroperoxybenzoic acid in refluxing chloroform is complete after 30 min (solution approximately 0.5 M in olefin and in peracid).